Volume 16, Number 4, 2023. pp. 475-482

Jordan Journal of Physics

ARTICLE

Estimating the Dimensions of the Radiological Field Suitable For the Treatment of Cancerous Tumors by Simulating a Proton Treatment System and Applying It to a Water Phantom Using the MCNP Code

Lara K. Jarouj[a], **Anis Bilal**[a] and **Nikola Abo Issa**[b]

[a] *Department of Physics, Faculty of Science, Al-Baath University, Syrian Arab Republic.*
[b] *Faculty of Biomedical Engineering, Damascus University, Syrian Arab Republic.*

Doi: https://doi.org/10.47011/16.4.10

Received on: 15/12/2021; *Accepted on: 21/03/2022*

Abstract: In this paper, the proton therapy system was simulated using the MCNPX code, and an analysis of the dimensions of the resulting radioactive field and dose distribution within the radiation field was conducted using the double beam scattering technique. The energy deposited in terms of depth was also studied within a water phantom with dimensions of $11\times11\times30\ cm^3$ divided into elemental volumes, each measuring $1x1x0.4\ cm^3$. This analysis was performed using a modified acceleration for range, where each cycle of the modified wheel was divided into 25 steps, with each step represented by an equivalent thickness of lead and Lexan. The study revealed the possibility of obtaining a radioactive field with dimensions of 7 x $7\ cm^2$, concentrating about 95% to 100% of the maximum dose. Additionally, it was also found that the dose distribution can extend to a depth of 20 cm within the phantom.

Keywords: Protons, MCNPX, Proton therapy system, Radiation dose.

1. Introduction

Protons are charged particles that deposit their energy in the medium through interactions. This is done according to several mechanisms, the most important of which are listed below [1].

- Collisions (collisional energy loss), where protons collide either with the electrons of the material or with the nucleus's colloidal potential (electromagnetic interactions). Additionally, protons can interact with the nuclear potential of the nucleus itself (nuclear interactions that are subject to the laws of strong mutual influence in the nucleus).
- Radiation (radiative energy loss), where the charged particles interact electromagnetically with the nucleus field, resulting in the emission of photons at the expense of the kinetic energy of the charged particle. This type of interaction does not play an important role in the energy loss of heavy charged particles, and its importance emerges only in the energy loss of light charged particles such as electrons.
- Inelastic collisions with atomic electrons.
- Inelastic collisions with nuclei.
- Elastic collisions with atomic electrons and nuclei.

Protons are heavy charged particles, so their path through the medium is straight, unlike electrons and positrons. The energy deposited over the distance *ds* is given by [2, 3, 4]:

$$\frac{dE}{\mathrm{ds}} = \frac{4\pi e^4 z^2}{m_o.V^2}\,\mathrm{N.Z.}\left[\ln\left(\frac{2.m_o.V^2}{I}\right) - ln(1-\beta^2) - \beta^2\right] \quad (1)$$

where *ze* is the charge of the proton, $V = \beta.c$ is the speed of protons, *N* is the density of the

Corresponding Author: Lara K. Jarouj **Email**: lara732827@gmail.com

medium (atoms/cm^3) with atomic number *Z*, and *I* is the ionization energy of the medium.

As observed from the previous equation, there is a constant decrease in the energy of the protons as they cross the medium. This decrease in the energy of the protons correlates with an increase in the amount of ionization occurring over one length.

The shape of the Bragg crest of protons is determined by the mean ionization of one length according to the following relationship [2, 5]:

$$I(r) = \int_r^{\infty} \frac{i(x-r)}{\alpha.\sqrt{\pi}} \times e^{-\left[\frac{x-R}{\alpha}\right]^2} dx \quad (2)$$

In the equation above, *r* represents the distance from the source, *x* is the range of the single proton, *i(x-r)* denotes specific ionization along the single-particle trajectory at distance (x-r) from the end of its trajectory, and α is the range straggling parameter.

After the depth at which the Bragg peak is formed, there are no ionization events, i.e. there is no energy deposited from protons within the tissue after the Bragg peak. In addition, the position of the peak follows the energy of the particles, and the depth of the peak within the tissue can be controlled by controlling the energy of the incoming protons [6].

2. Research Methodology

In this research, we adopted the Monte Carlo methods represented by the MCNP code in order to:

- Model the proton source.
- Model the modified acceleration range and the beam scatterer, in addition to the determinants of the radiation beam.
- Study the distribution of radiation dose and the rate of the absorbed dose with depth. To facilitate this, we utilized a water phantom divided into voxel elements, each with dimensions of 1×1×0.4 cm³. The overall dimensions of the phantom were 11×11×30 cm³.

2.1 Radiation Simulation Code (MCNPX Version) [7]

Monte Carlo methods belong to the realm of mathematical statistics and probability. These methods encompass a series of computational algorithms that rely on the repeated execution of random operations until a solution to a problem is obtained. Generally, the more iterations performed, the more accurate the results become.

The MCNP code (Monte Carlo N–Particle code) is one of the most famous computer codes that leverage Monte Carlo methods for the transport of radiation. This code is written in the Fortran language and offers a wide array of applications, including the study of radiation shielding for various radiation types (neutrons, photons, electrons), radiation detection, estimating detector efficiency, calculating particle counts at specific locations, determining particle flux at points, surfaces, or within a volume, as well as computing deposited energy, absorbed doses, and radiation exposure from different radiation sources. Additionally, MCNP can be used to calculate radioactivity levels for various materials and elements, among numerous other applications.

2.2 Calculation of the Dose Due to Protons

The code MCNPX allows calculating the dose in different ways [8]. In this study, we relied on calculating the dose with the counter energy F6, which gives the energy deposited in each cell attributed to each source particle and is expressed as:

$$DE\left(\frac{MeV}{g}\right) = W \times T_l \times \sigma_T(E) \times H(E) \times \frac{\rho_a}{m} \quad (3)$$

where:

W is the source weight, T_l is the particle track length (cm),

σT (E) is the total microscopic cross-section in barns,

H(E) is the heating number in MeV/collision,

ρ_a is the atomic density of the cell substance (atom /barn cm),

and m is the mass of the cell (g).

Using the above, the value of the absorbed dose in each cell, estimated in one (Gy = J/kg), can be calculated using the relationship:

$$D\left(\frac{Gy}{source\ particle}\right) = DE\left(\frac{MeV}{g}\right) \times 1.6 \times 10^{-13}\left(\frac{J}{MeV}\right) \times 10^3\ \left(\frac{g}{kg}\right) \quad (4)$$

3. The Computer Study Using the Code MCNPX

3.1 Simulation of the Proton Source (Cyclotron Accelerator)

A cyclotron is used to accelerate hydrogen ions, raising their energies within the range of 70 to 250 MeV, provided that the output intensity is not less than $1x10^{11}$ protons per second [9]. In this process, the electrons are removed from hydrogen atoms and injected into the accelerator.

As a consequence of these ions' rotation around the synchrotron, approximately 10,000 revolutions per minute occur within the accelerator tubes, which are maintained under a vacuum of 10-8atm. This environment facilitates the attainment of the specified ion energies.

The accelerator's output energy is determined based on the depth and location of the tumor within the tissue. For ocular tumors, protons with an energy of 70 MeV may be employed. With an increase in particle energy, the penetration depth of these particles within the tissue also increases.

3.2 Range-modified wheel (RMW)

It is necessary to distribute the maximum dose within a wide range to cover a wide area of the tumor, where the Prague peak for a single-energy proton beam is about 0.6 cm and is not sufficient to treat a large area of the tumor [10]. Thus, range modulation is used to create a set of spread-out Bragg peaks (SOBPs) that collectively cover the tumor area. This group of peaks is formed along the central axis of the treatment area through the modified wheel as shown in Fig. 1.

The range modulation wheel (RMW) consists of a number of sectors (Fig. 1) Each sector is made from various proton-absorbing materials with varying thicknesses, ranging from the least thickness at the start of the sector to the maximum thickness at its midpoint. The sectors are separated by equal spaces. When the wheel rotates, proton beams passing through the spaces between the segments generate Bragg peaks at the greatest depth within the tumor area. Conversely, proton beams passing through the segments themselves penetrate to lower depths within the tumor area. When the wheel rotates at a constant rate, Bragg peaks are generated at consistent intervals, starting from the beginning of the tumor region. At this point, protons pass through the maximum thickness of the wheel sector. The peaks continue to form until the greatest depth within the tumor is reached, corresponding to the passage of protons through the spaces between the wheel sectors.

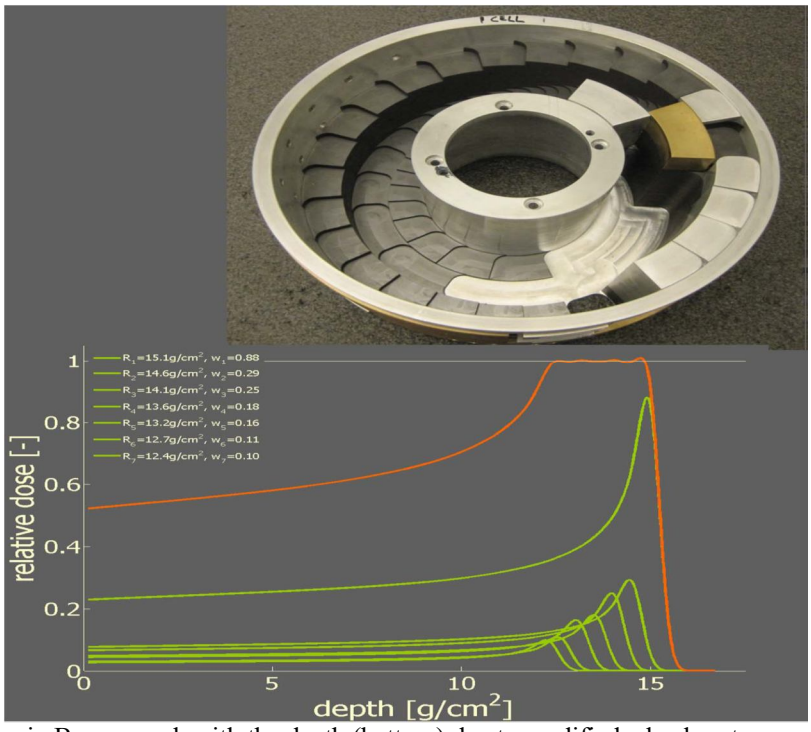

FIG. 1. The change in Braggs peak with the depth (bottom) due to modified wheel sectors corresponding to the source of protons (top) [11].

Given the limitation of studying the kinematics of the modified wheel within the MCNPX code, the simulation was carried out separately for each number of steps (25 steps) of the modified wheel. Subsequently, the results from these individual simulations were combined to obtain a set of Bragg peaks (SOBP), Table 1 shows the verified reference values for both lead and Lexan thicknesses used in the simulation of the modified wheel design at each step [10]. Fig. 2 shows the geometric design of the modified wheel in one step.

TABLE 1. The thickness of lead and Lexan used in the simulation of the design of the modified wheel at each step.

Step No.	Lead (cm)	Lexan (cm)	Step No.	Lead (cm)	Lexan (cm)
1	0.5390	0.0000	14	0.3424	10.4434
2	0.5278	0.7831	15	0.3227	11.2709
3	0.5154	1.5719	16	0.3021	12.1032
4	0.5024	2.3640	17	0.2805	12.9410
5	0.4889	3.1589	18	0.2578	13.7849
6	0.4749	3.9564	19	0.2337	14.6357
7	0.4603	4.7566	20	0.2082	15.4945
8	0.4453	5.5595	21	0.1809	16.3625
9	0.4297	6.3653	22	0.1517	17.2409
10	0.4135	7.1741	23	0.1199	18.1331
11	0.3967	7.9861	24	0.0850	19.0421
12	0.3793	8.8014	25	0.0456	19.9746
13	0.3612	9.6206			

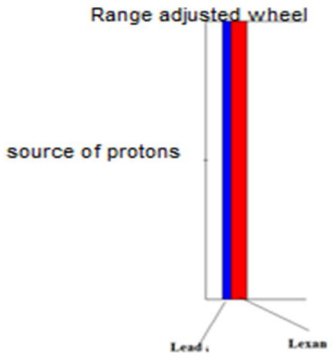

FIG. 2. Range-adjusted acceleration using the code MCNPX at one step.

3.3 Double Beam Scatter System

The double beam scatter system is composed of material with a high atomic number Z such as lead that gives the parallel proton beams emitted by the accelerator the shape of a cylindrical Gaussian in order to fit with the processing field, which typically measures 10x10 cm. Since the use of the single scattering is limited by the low yield, low beam energy of protons, and the small region of the energy deposition, correction is done using a double scatterer [10].

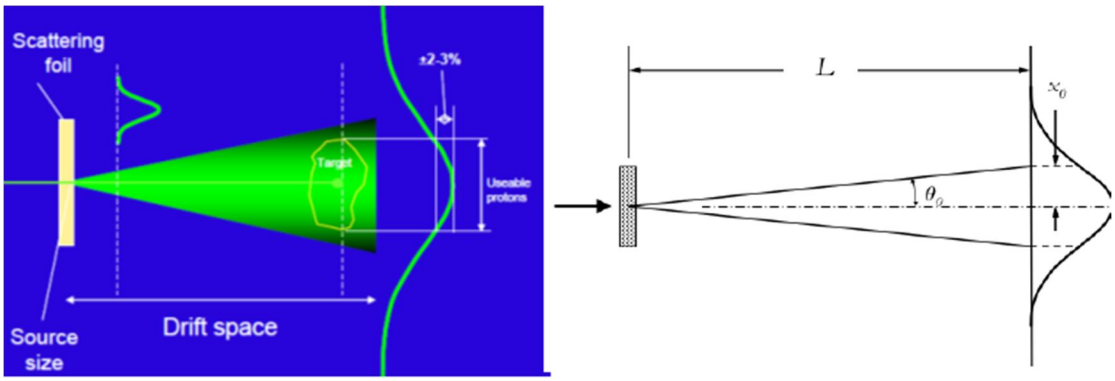

FIG. 3. The Gaussian distribution of the protons released by the band scatterer [9, 10].

The primary goal of the beam scatterer is to produce a radiation field wide enough to cover the entire area of the tumor. The compensating scatterer of the range (Range Compensated Scatterer) is also used to spread the Gaussian distribution of the proton beam and create a uniform and symmetric radiation field, which is designed to take the form of a diving distribution to produce a flat radiation beam in terms of energy consisting of two materials, lead and Lexan, as shown in Fig. 4.

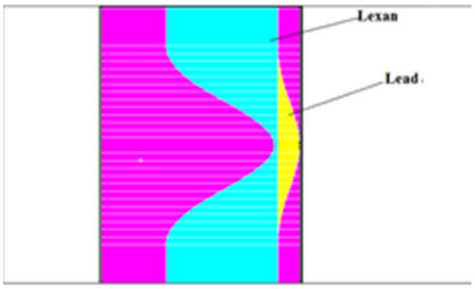

FIG. 4. Range Compensated Scatterer built using MCNPX.

3.4 Collimators and Final Aperture

In proton therapy usually one to four limiters made of copper alloys are used, Fig. 5.

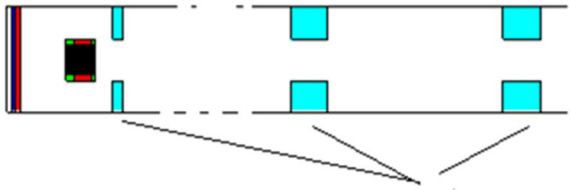

Determinants of the package and the final hypothesis

FIG. 5. Beam and final hypothesis determinants model using the code MCNPX.

3.5 Water Phantom

A water phantom was used in front of the outlet of the treatment system, divided into a number of voxel cells with dimensions of $1 \times 1 \times 0.4\ cm^3$per element. The dimensions of the phantom are $11 \times 11 \times 30\ cm^3$as shown in Fig. 6.

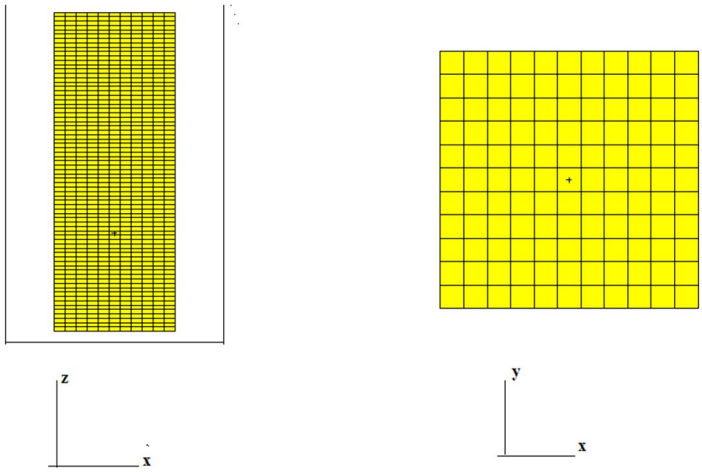

FIG. 6. The water phantom studied using the code MCNPX.

4. Results and Discussion

4.1 Changing the Dimensions of the Radiation Field

The proton therapy system was simulated using the MCNPX code. For each cycle of the modified wheel in the RMW range, as specified in Table 1, the code was executed. At each step of the simulation, the code ran for approximately one hour. Fig. 7 shows the radiation field and the percentage distribution of the radiation dose resulting from accelerated protons to 231 MeV energy with and without a range-compensated scatterer.

4.2 Changes in the Dose with the Number of the Range-adjusted Wheel

Fig. 9 shows the change of the energy deposited in terms of depth within the phantom for each step of the modified wheel.

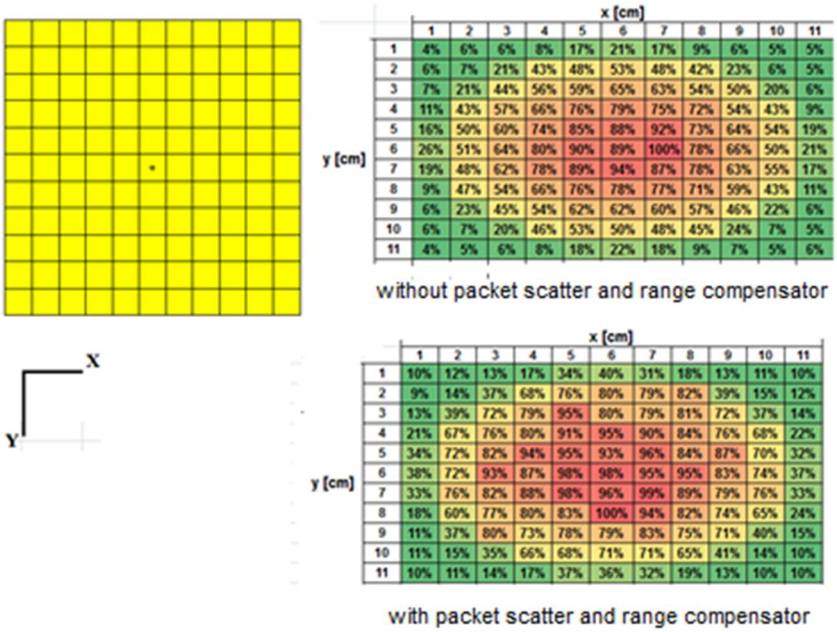

x [cm]

y [cm]	1	2	3	4	5	6	7	8	9	10	11
1	4%	6%	6%	8%	17%	21%	17%	9%	6%	5%	5%
2	6%	7%	21%	43%	48%	53%	48%	42%	23%	6%	5%
3	7%	21%	44%	56%	59%	65%	63%	54%	50%	20%	6%
4	11%	43%	57%	66%	76%	79%	75%	72%	54%	43%	9%
5	16%	50%	60%	74%	85%	88%	92%	73%	64%	54%	19%
6	26%	51%	64%	80%	90%	89%	100%	78%	66%	50%	21%
7	19%	48%	62%	78%	89%	94%	87%	78%	63%	55%	17%
8	9%	47%	54%	66%	76%	78%	77%	71%	59%	43%	11%
9	6%	23%	45%	54%	62%	62%	60%	57%	46%	22%	6%
10	6%	7%	20%	46%	53%	50%	48%	45%	24%	7%	5%
11	4%	5%	6%	8%	18%	22%	18%	9%	7%	5%	6%

without packet scatter and range compensator

X
Y

x [cm]

y [cm]	1	2	3	4	5	6	7	8	9	10	11
1	10%	12%	13%	17%	34%	40%	31%	18%	13%	11%	10%
2	9%	14%	37%	68%	76%	80%	79%	82%	39%	15%	12%
3	13%	39%	72%	79%	95%	80%	79%	81%	72%	37%	14%
4	21%	67%	76%	80%	91%	95%	90%	84%	76%	68%	22%
5	34%	72%	82%	94%	95%	93%	96%	84%	87%	70%	32%
6	38%	72%	93%	87%	98%	98%	95%	95%	83%	74%	37%
7	33%	76%	82%	88%	98%	96%	99%	89%	79%	76%	33%
8	18%	60%	77%	80%	83%	100%	94%	82%	74%	65%	24%
9	11%	37%	80%	73%	78%	79%	83%	75%	71%	40%	15%
10	11%	15%	35%	66%	68%	71%	71%	65%	41%	14%	10%
11	10%	11%	14%	17%	37%	36%	32%	19%	13%	10%	10%

with packet scatter and range compensator

FIG. 7. Radiation field and percentage distribution of radiation dose resulting from accelerated protons to 231 MeV energy with and without a range-compensated scatterer.

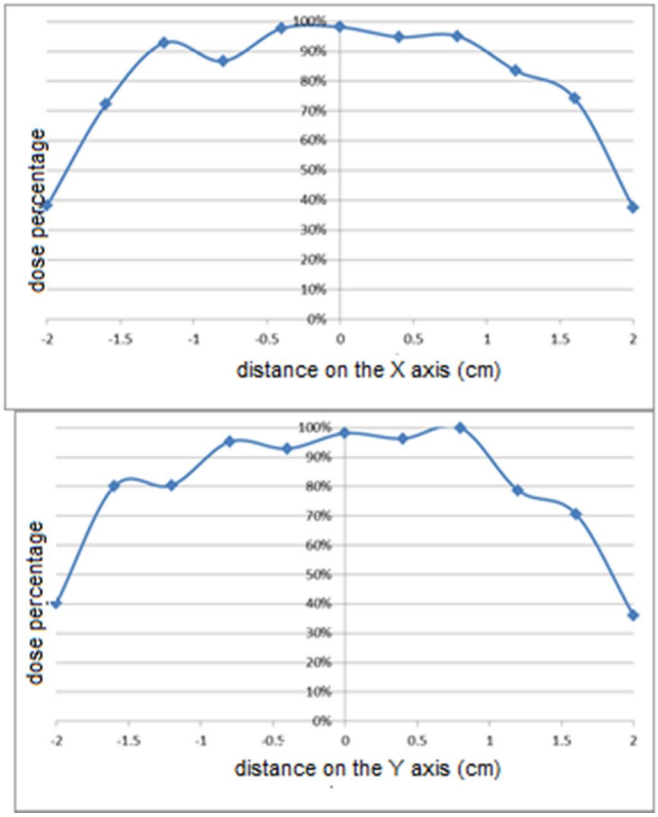

FIG. 8. The radiation field and the percentage distribution of the radiation dose resulting from accelerated protons to 231 MeV energy in the presence of a range-compensated scatterer on the x and y axes.

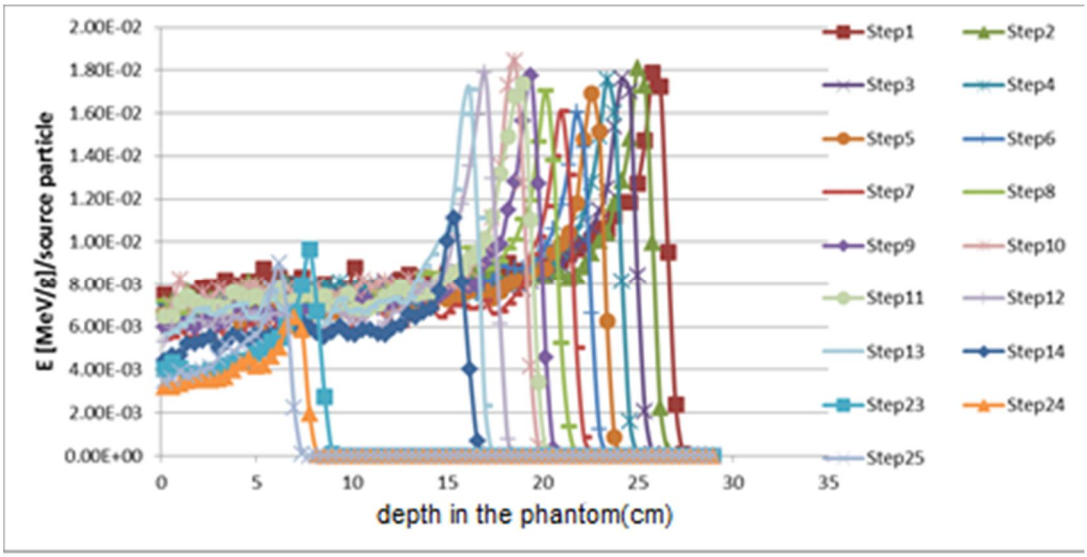

FIG. 9. Changes the energy deposited relative to each source particle as a function of depth within the phantom for each step of the modified acceleration.

4.3 Discussion

In this work, a beam of protons accelerated to 231MeV energy [10, 12] was used to simulate the radiation dose distribution within a water phantom using a proton treatment system.

The range-adjusted wheel was simulated using the code MCNPX after dividing each cycle into 25 steps (25 input files). The simulation also included the modeling of multiplier beam scatter.

Figs. 7 and 8 show the distribution of the radiation dose as a percentage of the maximum dose on the x and y axes with and without the use of a double beam scatterer. Fig. 7 illustrates that the use of a beam scatterer allows for the distribution of the maximum dose over a radiation field measuring approximately $7\times7cm^2$. In contrast, when a multiplexed beam scatterer is not employed, the radiation beam follows a divergent distribution and deposits all of its energy within a narrow radial field, no larger than 2x2 cm^2.

Fig. 9 shows the set of Bragg peaks (SOBP) generated within the phantom as a result of the rotation of the modified wheel for one cycle after dividing the cycle into 25 steps. The weaving pattern, which involves alternating between equivalent thicknesses of lead and Lexan, is given in Table 1. These simulations were conducted using accelerated protons with a constant energy. As we can see from Fig. 9, the maximum energy deposited is

$$1.7 \times 10^{-2} \left[\frac{MeV}{g}\right] / source\ particle$$

and using Eq. (4) we find that the value of the absorbed dose is about

$$D = 2.7 \times 10^{-12}\ [Gy] / source\ particle$$

References

[1] Smith, A.R., Phys. Med. Biol., 51 (2006) R491.

[2] Studenski, M.T. and Xiao, Y., World J. Radiol., 2 (4) (2010) 135-42.

[3] Akhtiar, A.M., "Biological Effects of Ionizing Radiation - Cancer", Master's lectures, Department of Physics - Faculty of Science - Damascus University, (2011).

[4] Martin, J.E., "Physics for Radiation Protection. A Handbook", (2006).

[5] Kjellberg, R.N. *et al.*, Trans. Am. Neurol. Assoc., 87 (1962) 216.

[6] Miller, D.W., Med. Phys., 22 (1995) 1943.

[7] Evaluation Subcommittee of ASTRO's Emerging Technologies Committee, "An Evaluation of Proton Beam Therapy", (American Society for Radiation Oncology, 2009).

[8]https://www.radiologyinfo.org/en/info/protonthera, accessed on: 27/12/2012.

[9] Butler, R., "The Patient Proton", (Chemistry Department, Norwich University, n.d).

[10] Ryckman, J.M., MS Thesis, Georgia Institute of Technology, (2011).

[11] Slopsema, R., "Intensity Modulated Proton Therapy", (University of Florida Proton Therapy Institute, August 5, 2011).

[12] Slater, J.M. *et al.*, Int. J. Radiat. Oncol., 22 (1991) 383.

[13] Jarouj, L.K., Al-Baath University Journal, 41 (2019).